THE JOURNAL OF BIOLOGICAL CHEMISTRY
Vol. 268, No. 33, Issue of November 25, pp. 25213-25220, 1993
Printed in U.S.A.

Calmodulin-Cardiac Troponin C Chimeras

EFFECTS OF DOMAIN EXCHANGE ON CALCIUM BINDING AND ENZYME ACTIVATION*

(Received for publication, April 1, 1993, and in revised form, July 14, 1993)

Samuel E. George‡, Zenghua Su, Daju Fan, and Anthony R. Means

From the Departments of Medicine and Pharmacology, Duke University Medical Center, Durham, North Carolina 27710

Calmodulin (CaM) and the cardiac isoform of troponin C (cTnC) are close structural homologs, but cTnC cannot activate most CaM target enzymes. To investigate structure-function relationships, we constructed a series of CaM·cTnC chimeras and determined their ability to bind Ca^{2+} and activate CaM target enzymes. Previously, we exchanged domain 1 and found that the chimeras exhibited profoundly impaired activation of smooth muscle myosin light chain kinase (smMLCK) and had differential effects on other CaM target enzymes (George, S. E., VanBerkum, M. F. A., Ono, T., Cook, R., Hanley, R. M., Putkey, J. A., and Means, A. R. (1990) *J. Biol. Chem.* 265, 9228–9235). One of the domain 1 chimeras was a potent competitive inhibitor of smMLCK. We now extend our study of CaM·cTnC chimeras by exchanging all of the remaining functional domains of CaM and cTnC. We determined the ability of the chimeras to bind Ca^{2+} and activate phosphodiesterase (PDE) and smMLCK. Chimeras containing both domains 3 and 4 of cTnC exhibited high affinity Ca^{2+} binding that was indistinguishable from cTnC, whereas chimeras containing either domain 3 or 4 of cTnC demonstrated Ca^{2+} affinity that was intermediate between CaM and cTnC. All of the CaM·cTnC chimeras showed near-maximal PDE activation but required 5–775-fold higher concentrations than CaM to produce half-maximal PDE activation. In contrast, all of the chimeras showed impaired ability to activate smMLCK, and some were potent competitive inhibitors of smMLCK activation by CaM.

Calmodulin (CaM)[1] is a ubiquitous intracellular Ca^{2+} receptor in eukaryotic cells. It participates in a number of intracellular Ca^{2+} signal transduction pathways through its ability to bind and activate a number of regulatory proteins and enzymes (reviewed in Ref. 1). Understanding the structural basis of CaM's interaction with its target enzymes is important to understanding how CaM accomplishes its diverse regulatory functions.

CaM is a 16.8-kDa protein that has four helix-loop-helix Ca^{2+} binding domains, termed EF-hands. These domains are paired in amino- and carboxyl-terminal globular domains, separated by a flexible 8-turn central helix (2–5). Upon complex formation with model binding peptides, CaM undergoes a striking structural rearrangement (6, 7). The central helix bends 100° and twists 120°, closely associating the two globular Ca^{2+} binding regions about a pseudo-2-fold axis of symmetry and enveloping the CaM-binding peptide in a hydrophobic tunnel. The surface of the complex is composed primarily of residues from the eight helical segments and the interhelix linker regions. The CaM-peptide complex structure does not reveal how the surface of CaM might interact with other functional domains of the CaM target enzyme.

Chimeras between CaM and a homologous calcium-binding protein, cardiac troponin C (cTnC), may help to define CaM-target enzyme interactions. The two proteins show remarkable structural similarity, with 50% amino acid identity (2, 8, 9). Although cTnC has not been crystallized, it has a high degree of sequence similarity with both CaM and the skeletal isoform of TnC (sTnC) (10). Therefore, it is likely that cTnC shares the dumbbell-shaped structure described for CaM and sTnC (2, 8, 9).

Despite its structural similarity to CaM, cTnC cannot activate CaM target enzymes (11, 12). By exchanging functional domains between the two, it should be possible to define regions of CaM that are essential for activation and cannot be substituted by corresponding domain of the inactive homolog, cTnC. The same approach may also be used to investigate other functional differences between CaM and cTnC, such as the higher Ca^{2+} affinity of cTnC's carboxyl-terminal domains (13–15). The information gained from a CaM·cTnC chimera study can then direct a more detailed mutagenesis study.

We used this approach to show that substitution of CaM's domain I had differential effects on CaM target enzymes (11). One CaM·cTnC chimera, TaM-BM1 (domain 1 of cTnC, domains 2–4 of CaM, with its inactive first domain restored by mutagenesis) activated some CaM target enzymes but proved to be a potent competitive antagonist of smooth muscle myosin light chain kinase (smMLCK) (11). The competitive inhibitor phenotype and additional data demonstrated that TaM-BM1 bound to smMLCK but failed to activate the enzyme. Further mutagenesis defined three residues in domain 1 of CaM that were essential for full activation of smMLCK, namely Glu-14, Thr-34, and Ser-38 (16). When these three CaM residues were mutated together, the resulting CaM triple mutant (E14A,T34K,S38M) reproduced the competitive inhibitor phenotype of TaM-BM1.

Here we extend our approach to the remaining functional domains of CaM. We construct and assay a new series of

* This work was supported by grants from the American Heart Association, Texas affiliate, the Methodist Hospital Foundation, Houston, Texas (to S. E. G.), and Public Health Service Grant GM-33976 (to A. R. M.). The costs of publication of this article were defrayed in part by the payment of page charges. This article must therefore be hereby marked "*advertisement*" in accordance with 18 U.S.C. Section 1734 solely to indicate this fact.

‡ Supported by a clinical investigator award from the National Heart, Lung, and Blood Institute. To whom correspondence should be addressed: Cardiovascular Division, Box 3060, Duke University Medical Center, Durham, NC 27710. Tel.: 919-681-8446; Fax: 919-684-8591.

[1] The abbreviations used are: CaM, calmodulin; MOPS, 3-(*N*-morpholino)propanesulfonic acid; DTT, dithiothreitol; PCR, polymerase chain reaction; cTnC, cardiac troponin C; PDE, calmodulin-stimulated cyclic nucleotide phosphodiesterase; smMLCK, smooth muscle myosin light chain kinase; bp, base pair(s).

CaM·cTnC chimeras, exchanging calcium binding domains 2, 3, and 4 and the central helices. Again we observe that domain exchange has differential effects on target enzymes and that some chimeras competitively inhibit CaM activation of smMLCK.

EXPERIMENTAL PROCEDURES

Construction of Chimeras

To exchange functional domains of CaM and cTnC, we added *Sac*I and *Sal*I sites to pCaMPL and a *Sal*I site to pTnCPL3 in the cDNA sequences that correspond to the amino acid residues indicated in Fig. 1. These restriction sites enabled us to exchange domains 3 and 4. For the central helix exchange, addition of restriction sites was impractical because of objectionable mutations. Instead, we used overlap extension PCR (17). The details of construction are in the following paragraphs.

pCaM[3,4 TnC], pTnC[3,4 CaM], and pTnC[3,4 CaM][BM1]—The bacterial expression plasmid pTnCPL3 (chicken cTnC) (18, 19) has a *Sac*I site (GAG CTC). A *Sac*I site was engineered into the corresponding position of pCaMPL. This mutates Ile-85 of CaM to Leu, which has no effect on Ca^{2+} binding or activation of the target enzymes presented here (data not shown). We call this mutant pCaM[*Sac*I]. The *Sac*I-*Nde*I restriction fragments were then exchanged between pCaM[*Sac*I] and pTnCPL3 to produce pCaM[3,4 TnC] and pTnC[3,4 CaM]. To make pTnC[3,4 CaM][BM1], the *Nco*I-*Sac*I fragment of pCBM1 (18) was subcloned into the corresponding site of pCaM[*Sac*I].

pCaM[2 TnC]—The expression plasmid pCaT encodes a CaM·cTnC chimera in which amino acid residues 1–47 (domain I) come from CaM, and amino acid residues 48–153 correspond to amino acid residues 57–161 (domain 2–4) of cTnC (11). To construct CaM[2 TnC], pCaT was amplified using PCR. The forward oligo(GAA TAC CAT GGC AGA TCA GCT GAC TGA GGA AAC) creates an *Nco*I site at the initiation codon and corresponds to the NH_2-terminal 8 amino acid residues of CaM. The reverse oligo(ACC CAG TCA CGT AGC GAT AGC, hereinafter oligo 2) lies 3′ to a convenient *Nde*I site in the expression plasmid. This PCR product is treated with proteinase K (20), agarose gel-purified, digested with *Nco*I and *Sac*I, and subcloned into a vector obtained by digesting pCaM[*Sac*I] with *Nco*I and *Sac*I. The resulting protein product contains amino acid residues 1–47 of CaM, 56–93 of cTnC, and 81–148 of CaM.

pTnC[2 CaM]—The expression plasmid pTaM encodes a CaM·cTnC chimera in which amino acid residues 1–56 (domain 1) are derived from cTnC and 57–157 correspond to 48–148 (domains 2–4) of CaM (11). We used PCR to amplify domains 1 and 2 of pTaM, designing the reverse oligo to incorporate a *Sac*I site at nucleotides 276–281. This PCR product is treated with proteinase K (20), agarose gel-purified, digested with *Nco*I and *Sac*I, and subcloned into a vector obtained by digesting pTnCPL3 with *Nco*I and *Sac*I. The resulting protein product contains amino acid residues 1–56 of cTnC, 48–80 of CaM, and 93–161 of cTnC.

pCaM[CH-TnC]—To construct this chimera, we used overlap extension PCR (17). In first stage PCR 1, pCaM[*Sac*I] is the template, the forward oligo is ACC ACA CCT ATG GTG TAT GC (oligo 3; lies 70-bp 5′ to the *Nco*I site/initiation codons of pCaMPL and pTnCPL3), and the reverse oligo is CCT TTG CTG TCA TCT TTC ATT TTC CTG GCC ATC ATG GTC. In first stage PCR 2, pTnC[3,4 CaM] is the template, the forward oligo is G ACC ATG ATG GCC AGG AAA ATG AAA GAT GAC AG, and the reverse oligo is oligo 2. The two first stage products are combined with oligos 2 and 3 in a second stage PCR. The second stage product is subcloned as described for pCaM[2 TnC]. This construction yields a protein product that is identical to CaM, except that residues 76–85 are replaced by residues 85–97 of cTnC (see Fig. 1; the exchange runs from the overlap extension splice point to the *Sac*I site).

pCaM[4 TnC] and pTnC[4 CaM]—Using overlap extension, a unique *Sal*I site was engineered between bp 364–370 of pCaM(*Sac*I) and between bp 398 and 403 of pTnCPL3. At the amino acid level, this results in conservative substitutions, I133V, E134D in pTnCPL3. The mutations in pCaM(*Sac*I) are silent.

pTnC[SalI]—The first stage PCR template is pTnCPL3. The overlap oligos for first stage PCR 1 and 2 are CAG TTC GTC GAC GAC ATC CTC AGT and GAG GAT GAC GTC GAC GAA CTG ATG, respectively. The outside oligos for first stage PCR 1 and 2 are oligo 3 and oligo 2, respectively.

pCaM[SalI]—The first stage PCR template is pCaM[*Sac*I]. The overlap oligos for first stage PCR 1 and 2 are GAA GAA GTC GAC GAA ATG ATT AGG and CAG TTC GTC GAC TTC TTC ATC

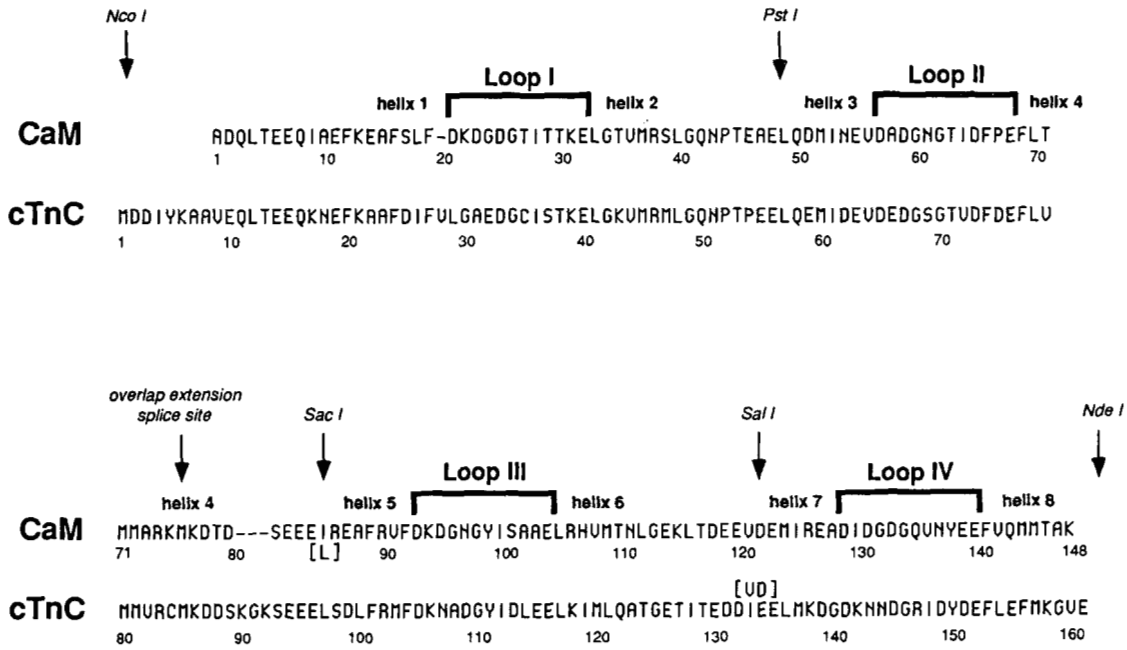

FIG. 1. **Amino acid sequences of CaM and cTnC, aligned to emphasize domain homology.** The restriction sites in the corresponding expression plasmids used to construct the chimeras are indicated above the sequences. The *Nco*I, *Pst*I, and *Nde*I sites were already present in the expression plasmids; the *Sac*I and *Sal*I sites were added as part of this study. The splice point for overlap extension is indicated (see text and "Experimental Procedures"). Also indicated are the residue numbers of CaM and cTnC beneath the sequences, the eight helical segments that comprise the four calcium binding domains of CaM and cTnC, the four 12-residue calcium binding loops bracketed above the sequences, and the conservative substitutions that resulted from the addition of restriction sites (in *brackets* immediately *above* or *below* the sequence).

TGT, respectively. The outside oligos are oligo 3 and oligo 2, respectively.

pCaM[4 TnC] and pTnC[4 CaM]—These are constructed by exchanging *Sal*I-*Nde*I restriction fragments between pTnC(*Sal*I) and pCaM(*Sal*I).

pCaM[3 TnC]—This was constructed by digesting pTnC[4 CaM] with *Sac*I and *Nde*I and subcloning the 805-bp restriction fragment into a *Sac*I-*Nde*I digested vector derived from pCaM[*Sac*I].

pTnC[3 CaM]—This was constructed by digesting pCaM[4 TnC] with *Sac*I and *Nde*I and subcloning the 404-bp restriction fragment into a *Sac*I-*Nde*I digested vector derived from pTnCPL3.

The above described inserts and vectors were ligated and used to transform *Escherichia coli* strain MM294 cI^+ using established techniques (21, 22). The desired mutant colony was identified by restriction mapping where feasible or by DNA sequencing. The DNA sequence of each expression plasmid was determined (Sequenase, U. S. Biochemical Corp.). Fig. 2 is a schematic diagram of the 10 chimeras constructed for this study.

Protein Expression and Purification

The chimeric expression plasmids were used to transform *E. coli* strain N5151, and the chimeric proteins were expressed by heat shock as described (11). CaM[3,4 TnC], TnC[3,4 CaM], TnC[3,4 CaM] [BM1], CaM[2 TnC], CaM[CH-TnC], and CaM[4 TnC] were purified as described (11), with the following modification. The final purification using ion-exchange high pressure liquid chromatography was eliminated. Instead, we added 3–5 gm of phenyl-Sepharose, equilibrated with 50 mM Tris-Cl, pH 7.0, 1 mM EDTA, 1 mM DTT to the EDTA eluate from the first phenyl-Sepharose column (typical volume 30–50 ml). The slurry was shaken at room temperature for 30–45 min, then aspirated to dryness through a Millipore RA filter, 5.0 μM pore size. The filtrate contained the chimeric protein, and contaminating proteins remained bound to the phenyl-Sepharose.

For final purification of CaM[3 TnC] we used a Mono Q 5/5 or Mono Q 10/10 (fast protein liquid chromatography) (Pharmacia LKB Biotechnology Inc.) ion-exchange column (20 mM Tris-Cl, pH 7.0, 1 mM DTT, 0.1 mM EDTA, 0–500 mM NaCl gradient). The protein eluted at 300–330 mM NaCl and was concentrated and desalted before further use.

TnC[2 CaM], TnC[3 CaM], and TnC[4 CaM] bound incompletely to phenyl-Sepharose in low salt solutions. Bacterial lysates containing these chimeras were bound to phenyl-Sepharose in 50 mM Tris-Cl, pH 7.5, 1 mM $CaCl_2$, 1 mM DTT, 400 mM ammonium sulfate and were eluted with 500 mM Tris-Cl, pH 7.5, 1 mM DTT, 1 mM EDTA. The EDTA eluates were then dialyzed overnight against 2 liters of 20 mM Tris-Cl, pH 7.0, 1 mM DTT, 0.1 mM EDTA, then purified over a Mono Q 5/5 column as described for CaM[3 TnC].

Calcium Binding by Equilibrium Dialysis—These studies were performed as described by George *et al.* (11).

Fluorescence Enhancement—Measurements were made at ambient temperature on a Shimadzu RF-5000 spectrofluorimeter, with an excitation wavelength of 278 nM and an emission wavelength scanned from 300 to 350 nM. Excitation and emission bandwidths were both 5 nM. Scan rate was set at very slow. The peak fluorescence at 307 nM is reported. Protein concentrations were adjusted to 0.1 mg/ml in 100 mM MOPS, pH 7.0, 150 mM KCl, 0.4 mM EGTA. 3 μl of a 10 mM $CaCl_2$ solution (prepared from a 100 mM standard solution) (Orion) were added in successive aliquots to 3 ml of protein solution. At least three separate fluorescence determinations were made with at least two different protein preparations; no significant variation in fluorescence data was observed between protein preparations. Data reported is the mean of three successive titrations ± standard errors as indicated in Fig. 4. Free calcium concentration was determined as described by VanBerkum and Means (23). Buffers were calibrated, and free calcium concentration was verified by titrating a 3-ml sample of 0.1 mg/ml CaM, 1 μM indo-1, in 100 mM MOPS, 150 mM KCl, 0.4 mM EGTA, with successive 3-μl aliquots of 10 mM $CaCl_2$. The calibration sample was excited at 355 nM, and emission was scanned from 380 to 550 nM. Free Ca^{2+} was estimated from the ratio of fluorescence at 404 nM to fluorescence at 485 nM (24).

The fluorescence data was fit to one- and two-site models of the nonlinear Hill equation

$$y = \frac{y_{max1}}{1 + 10^{(n1(pCa50 - pCa))}} + \frac{y_{max2}}{1 + 10^{(n2(pCa50 - pCa))}}$$

where y = percent of maximal enhancement observed at a particular pCa; the subscripts 1 and 2 indicate phases 1 and 2 of the enhancement titration; y_{max}, maximal percentage enhancement observed in that phase of the titration; n, Hill coefficient; pCa50, negative logarithm of free Ca^{2+} concentration producing half-maximal enhancement in the indicated phase of the titration; pCa, negative logarithm of free Ca^{2+} concentration producing y percent of maximal enhancement. The one-site model excludes terms with the subscript 2. The curves were fit with a least squares nonlinear regression algorithm (Marquart algorithm, Kaleidagraph 3.0, Synergy Software, Reading PA). The selection of either the one- or two-site model was made by comparison of chi-square values and correlation coefficients between the two models and visual comparison of curve fits. The one-site model was selected for all fluorescence enhancement data except for CaM[3 TnC] and TnC[4 CaM], for which the two-site model was chosen.

Enzyme Assays

Phosphodiesterase Assays—Calmodulin-deficient phosphodiesterase was purified from rat brain, and phosphodiesterase activity was assayed as described by Putkey *et al.* (25). We also determined phosphodiesterase activity as a function of free calcium concentration, for CaM, CaM[3 TnC], and CaM[4 TnC]. For these studies, we made a series of 20 reaction buffers, containing 100 mM MOPS, pH 7.4, 150 mM KCl, 0.4 mM EGTA, 0.1 mM magnesium acetate, and increasing amounts of $CaCl_2$ to give the desired free $CaCl_2$ concentration (from pCa 8 through pCa 5 in 20 increments). We assayed CaM, CaM[3 TnC], or CaM[4 TnC] (500 nM) in each of the 20 buffers. Three separate experiments were performed, each in duplicate. The data was fit to a one-site nonlinear Hill equation as described above for the fluorescence enhancement data, and the mean pCa50 was determined. Standard errors for these pCa50 determinations were ± 0.2 pCa units or less.

Myosin Light Chain Kinase Assays—These were performed as described by VanBerkum and Means (16). Evaluation of chimeras as inhibitors was performed as described by George *et al.* (11) and VanBerkum and Means (16).

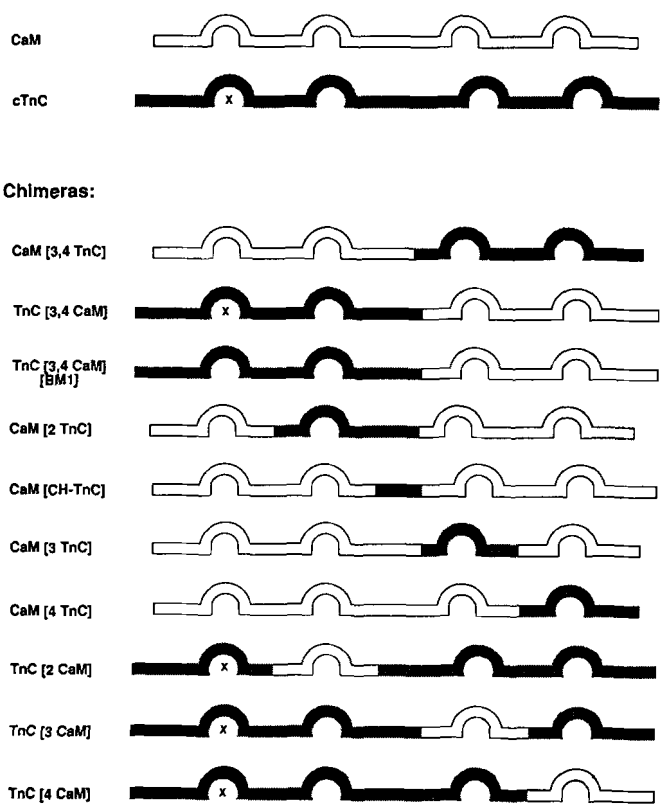

FIG. 2. **Diagram of CaM·cTnC chimeras.** CaM sequences are white, and cTnC sequences are gray. The four Ca^{2+} binding loops are shown as *semicircles*; an "*x*" inside the semicircle indicates the loop is unable to bind Ca^{2+}.

RESULTS

Construction, Expression, and Purification of the Chimeras—Construction of expression plasmids encoding 10 CaM·cTnC chimeras is detailed under "Experimental Procedures." A schematic diagram of the chimeras is shown in Fig. 2. The chimeras were expressed in *E. coli* and purified using hydrophobic affinity chromatography or hydrophobic affinity and ion-exchange chromatography (see "Experimental Procedures"). An SDS-polyacrylamide gel of the purified proteins is shown in Fig. 3.

Calcium Binding Properties—We used equilibrium dialysis to determine calcium binding properties of the CaM·cTnC chimeras (Table I). At *p*Ca 4, chimeras that have four functional Ca^{2+} binding domains bound approximately 4 Ca^{2+}/mol of protein (range, 3.7–4.4 mol of Ca^{2+} bound/mol of protein), whereas those with three functional domains bound approximately 3 mol of Ca^{2+}/mol of protein (range, 2.7–3.2 mol of Ca^{2+}/mol of protein).

At low free Ca^{2+} concentrations, the presence of domain 3 and/or 4 of cTnC had a significant effect on Ca^{2+} binding (see Table I, at *p*Ca 7–5.5). Constructs that contain both domains 3 and 4 of cTnC bind more Ca^{2+} than constructs containing the corresponding domains of CaM (compare *e.g.* CaM and TnC[3, 4 CaM] with TnC and CaM[3, 4 TnC]). Constructs that contain either domain 3 or 4 of cTnC demonstrate intermediate calcium affinity (compare *e.g.* CaM[3 TnC] with CaM and CaM[3, 4 TnC]).

To evaluate Ca^{2+} affinity with greater resolution, we studied fluorescence enhancement of the chimeras in response to incremental additions of Ca^{2+}. Both CaM and cTnC contain one tyrosine residue in calcium binding loop 3 and one in loop 4 (residues 99 and 138 of CaM and 111 and 150 of cTnC; cTnC contains a third tyrosine, at position 5 near the NH_2 terminus). Titration of CaM and cTnC with Ca^{2+} results in fluorescence enhancement, which reflects Ca^{2+}-dependent alterations in the tertiary structure (13, 14). Relative to CaM, Ca^{2+} titration of cTnC produces enhancement at about 1 log lower free Ca^{2+} concentration.

Fluorescence enhancement of CaM, cTnC, and the chimeras are presented in Fig. 4 and Table II. The fluorescence enhancement curves of cTnC and CaM[3,4 TnC] are nearly identical to each other (Fig. 4, *top*; *p*Ca50 7.2 and 7.1, respectively). Similarly, the enhancement curves of TnC[3,4 CaM] and CaM are nearly identical (*p*Ca50 6.1 and 6.0, respectively). Fluorescence enhancement with these proteins appears monophasic and exhibits strong positive cooperativity (Hill coefficients, 1.5–2.4).

The fluorescence enhancement data obtained for TnC[4 CaM] and CaM[3 TnC] show a rightward shift, relative to cTnC. Moreover, these chimeras appear to have biphasic fluorescence titrations (pCa_{50} 7.2 for cTnC *versus* 6.9 and 5.7 for both chimeras; see Fig. 4, *bottom* and Table II). For CaM[3 TnC], the second phase represents about 30–35% of the total enhancement and centers at *p*Ca50 5.7. Although TnC[4 CaM] also fits reasonably well to the single-site model of the nonlinear Hill equation, the two-site model appeared to give a better fit to the data between *p*Ca 6.3–5.0. If TnC[4 CaM] has a second phase, it represents about 15% of the total enhancement and like CaM[3 TnC] has a *p*Ca50 of 5.7. The Hill coefficients for these two chimeras range from 0.8 to 1.3, substantially lower than the other proteins reported here. Within observed error, these Hill coefficients do not suggest cooperativity (26, 27).

The fluorescence enhancement curves obtained with TnC[3 CaM] and CaM[4 TnC] appear monophasic and are left-shifted relative to CaM (pCa_{50} 6.0 for CaM *versus* 6.3 for both chimeras). CaM[2 TnC] and CaM[CH-TnC] are virtually identical to CaM, and TnC[2 CaM] is virtually identical to cTnC (data not shown).

Phosphodiesterase Assays—We studied the ability of CaM·cTnC chimeras to activate Ca^{2+}-CaM-dependent phosphodiesterase (Table III). In the assay, Ca^{2+}-CaM stimulates PDE activity 8–10 fold (11, 23). Although cTnC stimulates PDE activity to the same maximal extent as CaM, a very high concentration of cTnC is required before activation is observed. All of the CaM·cTnC chimeras activate PDE, but compared with CaM, higher concentrations of the chimeras are required to activate (*i.e.* all chimeras show increases in K_{act}, relative to CaM). Of the half-CaM, half-cTnC chimeras, CaM[3,4 TnC] shows the largest increase in K_{act} (about 300-fold). This increase is largely traceable to the presence of domain 3 of cTnC. CaM[3 TnC] shows a 133-fold K_{act} increase, whereas CaM[4 TnC] shows only an 9.5-fold K_{act} increase. In contrast, TnC[3,4 CaM] and TnC[3,4 CaM][BM1] show only about 6-fold K_{act} increases. CaM[2 TnC] and CaM[CH-TnC] also show only small K_{act} increases (6.3- and 4.6-fold, respectively). TnC[2 CaM], TnC[3 CaM], and TnC[4 CaM] all show substantial increases in K_{act}.

We questioned whether the apparent higher Ca^{2+} affinity of some CaM·cTnC chimeras might result in altered Ca^{2+} dependence of enzyme activation. To address this question,

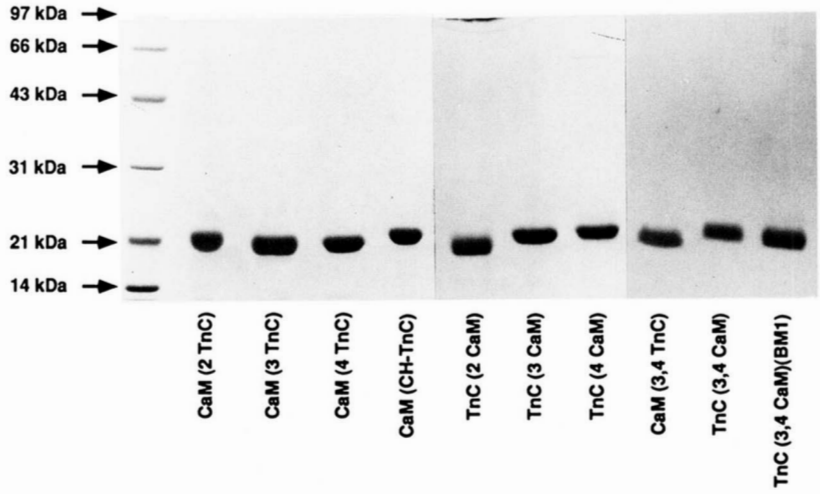

FIG. 3. **SDS-polyacrylamide gels of CaM·cTnC chimeras.** 15% SDS-polyacrylamide gel of the chimeras run in buffer containing 5 mM EDTA. 10 μg of each protein was loaded. The chimeras remain as single bands when lesser amounts are run. The chimeras undergo typical shifts toward lower apparent molecular weights when run in Ca^{2+} containing buffer (not shown).

TABLE I

Calcium binding to CaM·cTnC chimeric proteins

Extent of Ca^{2+} bound, expressed as mol of Ca^{2+} bound/mol of protein at the indicated *p*Ca. Determinations were made by equilibrium dialysis of chimeras as described under "Experimental Procedures." Data presented are the mean of two experiments done in triplicate ± standard error. Where no value is reported, the Ca^{2+} binding of the chimera was not determined at that *p*Ca.

	*p*Ca 7	*p*Ca 6.5	*p*Ca 6	*p*Ca 5.5	*p*Ca 5	*p*Ca 4
CaM	0.4 ± 0.2	0.5 ± 0.2	0.6 ± 0.1	1.4 ± 0.1	2.2 ± 0.2	4.1 ± 0.1
cTnC	1.0 ± 0.2	1.4 ± 0.1	1.8 ± 0.2	2.1 ± 0.1	2.8 ± 0.1	3.2 ± 0.2
CaM(3,4 TnC)	0.8 ± 0.2	1.1 ± 0.3	2.2 ± 0.2	2.0 ± 0.1	3.1 ± 0.2	4.2 ± 0.2
TnC(3,4 CaM)	0.2 ± 0.1	0.5 ± 0.2	0.9 ± 0.2	1.4 ± 0.2	2.3 ± 0.4	2.7 ± 0.1
TnC(3,4 CaM)(BM1)	0.4 ± 0.2	0.4 ± 0.2	0.5 ± 0.1	1.2 ± 0.3	2.1 ± 0.1	3.7 ± 0.2
CaM(3 TnC)	0.2 ± 0.1	0.8 ± 0.1	1.6 ± 0.2	1.9 ± 0.1	2.4 ± 0.1	3.7 ± 0.3
CaM(4 TnC)	0.2 ± 0.1	0.7 ± 0.2	1.1 ± 0.2	1.7 ± 0.1	2.3 ± 0.2	3.8 ± 0.2
CaM(2 TnC)						3.7 ± 0.1
TnC(2 CaM)						2.7 ± 0.3
TnC(3 CaM)						2.8 ± 0.4
TnC(4 CaM)						2.7 ± 0.2
CaM(CH-TnC)						4.4 ± 0.2

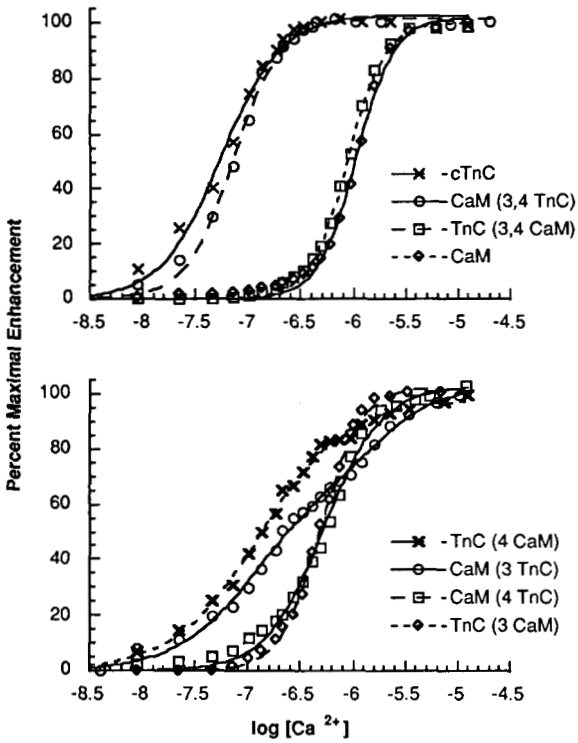

FIG. 4. **Fluorescence enhancement.** Changes in peak fluorescence were monitored as a function of log-free Ca^{2+} concentration. Data are expressed as percent of maximal fluorescence enhancement obtained between *p*Ca 8.5 and 4.5 for that protein. Curves were fit to a one- or two-site model of the nonlinear Hill equation, as described under "Experimental Procedures." *Top*, fluorescence enhancement of CaM, cTnC, and half-CaM, half-cTnC chimeras. *Bottom*, fluorescence enhancement of single-domain chimeras. *Abscissas* of the *top* and *bottom* graphs are aligned to allow comparison between the figures.

we studied PDE activation as a function of free Ca^{2+} concentration. At 100 nM CaM, the free Ca^{2+} concentration required to produce half-maximal fluorescence enhancement was considerably more than that required to produce half-maximal PDE activation (pCa_{50} of 6.0 for fluorescence enhancement *versus* pCa_{50} of 6.6 for PDE activation; see Tables II and III). The enhanced Ca^{2+} affinity of CaM[4 TnC] does not produce a lower Ca^{2+} requirement for PDE activation; both PDE activation and fluorescence enhancement have a *p*Ca50 of 6.3. For CaM[3 TnC], this effect was even more striking; the *p*Ca50 for PDE activation was 5.7. Thus, the apparent higher Ca^{2+} affinity of the chimeras relative to CaM does not produce

TABLE II

Summary of parameters observed in the fluorescence enhancement experiments

Fold enhancement is fluorescence observed at *p*Ca 4.5 divided by fluorescence observed at *p*Ca 8.5; $pCa50_1$ (and $pCa50_2$, where reported) refers to the *p*Ca at which enhancement was half-maximal. $Hill_1$ (and $Hill_2$, where reported) indicate the Hill coefficient for that phase of enhancement. Data reported are the mean of three successive titrations. Standard errors for determination of *p*Ca50s were ±0.1 *p*Ca units or less, for fold enhancement, ±0.1 or less, and for $Hill_1$, ±0.1 or less. The standard errors for both reported $Hill_2$ coefficients are ± 0.2.

	Fold enhancement	$pCa50_1$	$Hill_1$	$pCa50_2$	$Hill_2$
CaM	2.3	6.0	2.4		
cTnC	1.4	7.3	1.5		
TnC[3,4 CaM]	2.1	6.1	2.4		
CaM[3,4 TnC]	1.4	7.1	1.9		
CaM[3 TnC]	1.6	6.9	1.1	5.7	1.3
CaM[4 TnC]	1.8	6.3	1.6		
TnC[3 CaM]	1.4	6.3	2.3		
TnC[4 CaM]	1.4	6.9	1.1	5.7	0.8

TABLE III

Activation of calmodulin-dependent phosphodiesterase by CaM·cTnC chimeras

K_{act} is the protein concentration producing half-maximal PDE activation. Percent maximal activation is the percent of activation produced by saturating amounts of the protein (ranging from 100 nM for CaM to 5 μM for cTnC), divided by the activation produced by 100 nM CaM, multiplied by 100. Relative K_{act} is calculated by dividing the K_{act} by the K_{act} for CaM (2.0 nM). *p*Ca50 for PDE activation is the negative logarithm of the free Ca^{2+} concentration producing half-maximal PDE activation, with maximal PDE activation defined as that produced by 500 nM CaM at *p*Ca 4.0.

	K_{act}	Percent maximal activation	Relative K_{act}	*p*Ca50 for PDE activation
	nM			
CaM	2.0	100	1	6.6
cTnC	3900	98	1950	
CaM(3,4 TnC)	595	92	298	
TnC(3,4 CaM)	11.9	109	6.0	
TnC(3,4 CaM)(BM1)	13.0	99	6.5	
CaM(2 TnC)	12.5	102	6.3	
CaM(3 TnC)	265	96	133	5.7
CaM(4 TnC)	19	111	9.5	6.3
CaM(CH-TnC)	9.1	100	4.6	
TnC(2 CaM)	1420	96	710	
TnC(3 CaM)	360	93	180	
TnC(4 CaM)	1550	98	775	

PDE activation at lower free Ca^{2+} concentrations.

Smooth Muscle Myosin Light Chain Kinase Assays—Six of the 10 chimeras failed to activate smMLCK, even at concentrations as high as 5 μM (Table III). CaM[2 TnC], CaM[4 TnC], and TnC[3 CaM] retained some ability to activate smMLCK. CaM[2 TnC] reached 48% of the maximal activation produced by CaM, with a similar K_{act}. CaM[4 TnC] and TnC[3 CaM] were minimal activators but required substantially higher concentrations than CaM before activation was observed (K_{act}, 30 and >600 nM, respectively). In contrast to the other chimeras, CaM (CH-TnC) was an excellent activator of smMLCK. It achieved 85% of maximal smMLCK activation, with less than a 3-fold rightward K_{act} shift relative to CaM.

We assayed the 6 nonactivating chimeras for ability to inhibit smMLCK activation by CaM. The results are shown in Table IV. Screening of CaM[4 TnC], TnC[2 CaM], TnC[3 CaM], and TnC[4 CaM] indicated that they had some ability to inhibit but with K_is in the micromolar range. They were not evaluated further as inhibitors. In contrast, TnC[3,4 CaM], TnC[3,4 CaM][BM1], CaM[3,4 TnC], and CaM[3 TnC] showed significant competitive inhibition. The K_is ranged from 31–95 nM, comparable with the K_is observed for the domain 1 chimera TaM-BM1 (66 nM) and the CaM domain 1 triple mutant, E14A,T34K,S38 M (38 nM) (11, 16).

DISCUSSION

In the calmodulin superfamily, the EF-hand pair forms the fundamental unit of high affinity Ca^{2+} binding (9, 28). Despite their common secondary structural motifs, the Ca^{2+} binding affinity of EF-hand pairs varies by at least 3 orders of magnitude (28). Although several groups have proposed structure-function relationships (29–35), the mechanisms through which structural variations modulate binding affinity remain incompletely defined. Because the carboxyl-terminal EF-hand pair from cTnC binds Ca^{2+} with relatively high affinity ($K_d \approx 10^{-7}$) (13, 36, 37) and the corresponding region of CaM binds Ca^{2+} with intermediate affinity ($K_d \approx 10^{-5}$ to 10^{-6} M) (14, 38, 39), domain exchange between these regions of CaM and cTnC has the potential to provide additional relevant evidence about the structural basis of Ca^{2+} binding.

CaM[3,4 TnC] and cTnC both demonstrate relatively high affinity binding typical of the carboxyl-terminal domains of cTnC (13, 36, 37). In the lower range of Ca^{2+} concentrations, all constructs containing domains 3 and 4 of CaM bind significantly less Ca^{2+} than constructs containing domains 3 and 4 of cTnC. These data reflect the relatively low affinity of the carboxyl-terminal domains of CaM (14, 38, 39) and suggest that the factors that determine relative Ca^{2+} affinities are found within the EF-hand pair itself. An alternative possibility is that significant Ca^{2+} binding interactions exist between amino- and carboxyl-terminal domains, but it is not important whether the amino-terminal domains come from CaM or cTnC. However, data obtained with proteolytic fragments of CaM and TnC suggest that interactions between the amino- and carboxyl-terminal halves of the molecule do not substantially influence Ca^{2+} affinity (39, 40).

Our data indicate that the primary region responsible for the higher affinity of cTnC is domain 3. The carboxyl-terminal halves of CaM[3 TnC] and TnC[4 CaM] include domain 3 of cTnC and domain 4 of CaM; both have a *p*Ca50 at 6.9. The carboxyl-terminal halves of CaM[4 TnC] and TnC[3 CaM] include domain 3 of CaM and domain 4 of cTnC; both have a *p*Ca50 at 6.3. Thus, domain 3 of cTnC dictates a higher *p*Ca50 for fluorescence enhancement than domain 4. However, domain 4 is not without effect. CaM[4 TnC] and TnC[3 CaM] have higher *p*Ca50s than CaM (6.3 for the chimeras *versus* 6.0 for CaM), and TnC[4 CaM] and CaM[3 TnC] have lower *p*Ca50s than cTnC (6.9 for the chimeras *versus* 7.3 for cTnC).

The biphasic nature of the fluorescence titration of CaM[3 TnC] is noteworthy. A possible interpretation is that the first phase reflects Ca^{2+} binding to domain 3 of cTnC, and the second phase reflects Ca^{2+} binding to domain 4 of CaM. The clear division into two phases may be attributable to the relatively large difference in Ca^{2+} affinity between the two domains. There may also be disruption of domain 3-domain 4 interactions that enhance Ca^{2+} affinity and positive cooperativity in cTnC but are lost in the chimera. Unlike Ca^{2+} binding to CaM[3 TnC], TnC[4 CaM] cannot be unequivocally divided into two phases. This may be due to a relatively small second phase, which accounts for only 15% of the total enhancement and results in an equally good fit to either the one- or two-site model of the nonlinear Hill equation. If the two-site equation is correct for TnC[4 CaM], it produces *p*Ca50s of 6.9 and 5.7, which are the same as those observed for CaM[3 TnC].

The brain isoforms of CaM-stimulated PDE exist in solution as dimers of 61- or 59-kDa subunits (41–43). Their activity is stimulated about 8–14-fold by Ca^{2+}-CaM, and the stimulation exhibits strong positive cooperativity. Generally, CaM mutants and chemically modified CaM derivatives maintain relatively normal ability to activate PDE but show variable K_{act} shifts that are thought to reflect impaired interaction between PDE and the modified CaM (11, 23, 25, 44–47). We showed previously that cTnC fully activated PDE, with a marked rightward K_{act} shift. A chimera with the first domain of cTnC and the last 3 domains of CaM was indistinguishable from CaM as a PDE activator, indicating that the first domain of cTnC is not responsible for its K_{act} shift (11). Thus, the structural basis of the K_{act} shift demonstrated by cTnC must exist somewhere in domains 2–4. The chimera data presented here allow one to localize the regions responsible for this marked rightward K_{act} shift. Of the single domain chimeras, CaM[3 TnC] exhibits the largest K_{act} shift; therefore, the bulk of shift may be attributed to domain 3 differences. Differences in domain 2, the central helix, and domain 4 also contribute to K_{act} shift, but their contribution to the overall effect is substantially smaller than that of domain 3.

Some chimeras exhibit enhanced Ca^{2+} affinity, but the

TABLE IV

Activation and competitive inhibition of smMLCK by CaM·cTnC chimeras

Summary table. Assays and data analysis were performed as described under "Experimental Procedures." % max activation is the observed maximal activation of the chimera, divided by the activation observed with 100 nM CaM, multiplied by 100. K_{act} and K_i are the concentrations producing half-maximal activation and half-maximal inhibition, respectively.

Protein	% max activation	K_{act} (nM)	K_i (nM)
CaM	100	0.7	
cTnC	0		>2000
CaM(3,4 TnC)	0		38 ± 3
TnC(3,4 CaM)	0		95 ± 3
TnC(3,4 CaM)(BM1)	0		31 ± 2
CaM(2 TnC)	48 ± 2	0.5	Not tested
CaM(3 TnC)	0		42 ± 6
CaM(4 TnC)	12 ± 1	30	>600
CaM(CH-TnC)	85 ± 3	1.9	Not tested
TnC(2 CaM)	0		>600
TnC(3 CaM)	7 ± 2	>600	>600
TnC(4 CaM)	0		>600

enhanced affinity does not in turn produce enzyme activation at lower Ca^{2+} concentrations. The activation of CaM-dependent enzymes can be described by a general model involving the sequential binding of Ca^{2+} to CaM and multiple equilibrium reactions between the enzyme and various Ca^{2+}·CaM complexes (42, 48). Our data are consistent with this model. Although some chimeras exhibit enhanced Ca^{2+} affinity, the substitution of cTnC sequences for CaM sequences results in reduced affinity for PDE. Thus, despite their increased Ca^{2+} affinity in the absence of enzyme, the chimeras exhibit an increased Ca^{2+} requirement for PDE activation.

Calmodulin forms an extensive interface with smMLCK. In crystal structure, 32 CaM residues form about 185 contacts with a CaM-binding peptide derived from residues 796–815 of smMLCK (6). This produces a hydrophobic tunnel that envelops the entire length of the peptide. The 32 CaM residues involved in peptide binding extend from Glu-7 to Met-145 and involve all four EF-hand domains of CaM. In light of this structure, it is not surprising that CaM domain substitution significantly impairs smMLCK activation. The data we present here and elsewhere (11) show that all four CaM domains contain important smMLCK activating residues.

Not all of the activating residues are involved in binding smMLCK residues 796–815. For example, VanBerkum and Means (16) established that Glu-14, Thr-34, and Ser-38 play an important role in smMLCK activation. Only one of these residues, Glu-14, is involved in peptide binding; Thr-34 and Ser-38 lie on the solvent-exposed face of helix 2 and have no discernible contact with the smMLCK CaM-binding peptide. Therefore, Thr-34 and Ser-38 must interact with smMLCK in a region distinct from residues 796–815. Mutation of Thr-34 to lysine or Ser-38 to methionine did not prevent the formation of a stable enzyme-activator complex but did alter additional interactions that were essential for activation. If a sufficient number of these mutations were combined in a single molecule, the protein was a potent competitive inhibitor of smMLCK activation by CaM. The first domain cTnC·CaM chimera, TaM-BM1, and the CaM first domain triple mutant, E14A,T34K,S38, are examples of this competitive inhibitor phenotype.

The competitive inhibitor phenotype is not confined to chimeras and mutants involving domain I of CaM. All three of the half-CaM, half-cTnC chimeras are competitive inhibitors. TnC[3,4 CaM] is the least potent of the three (K_i = 95 nM), but restoration of the inactive first domain of this chimera (TnC[3, 4 CaM][BM1]) reduces its K_i to the lowest yet described for this class of inhibitors (31 nM). This result indicates that a functional first domain is not essential for the inhibitory phenotype but does enhance inhibitory potency. It is also noteworthy that TnC[3,4 CaM][BM1] has about a 2-fold lower K_i than does TaM-BM1 (11). The two constructs differ only in the origin of their second domains and central helices. Therefore, the enhanced inhibitory potency of TnC[3,4 CaM][BM1], relative to TaM-BM1, may be due to the absence of important activating residues in domain 2 and/or the central helix. This view is supported by the observation that CaM[2 TnC] and CaM[CH-TnC] do not fully activate smMLCK. Finally, a nonactivating phenotype does not necessarily imply a competitive inhibitor phenotype; TnC[2 CaM] and TnC[4 CaM] are nonactivators that show little ability to inhibit smMLCK activation.

The complete absence of smMLCK activation by CaM[3 TnC] documents that domain 3 of CaM plays a critical role in smMLCK activation. Our observations indicate that essential activating residues, analogous to Glu-14, Thr-34, and Ser-38, are likely to be found in domain 3 of CaM. Domain 3 is composed of helix 5 (Ile-85 to Phe-92) loop 3 (Asp-93 to Glu-104), and helix 6 (Ala-102 to Leu-112). The swap that produced CaM[3 TnC] also includes the helix 6-helix 7 linker region (Gly-113 to Val-121). Because CaM[CH-TnC] shows near maximal smMLCK activation, exchange of helix 5 cannot explain the inability of CaM[3 TnC] to activate. There are four nonconserved residues between the third loops of CaM and cTnC. Because three of these are directly involved in Ca^{2+} coordination (Asp-95, Asn-97, and Ser-101 in CaM loop 3; asparagine, aspartic acid, and aspartic acid, respectively, in the corresponding positions of cTnC) (2, 9), it is unlikely that they would interact directly with CaM target enzymes. Consequently, our data suggest that the critical smMLCK activating residues present in domain 3 of CaM may be located in helix 6 or the 6–7 linker.

Whereas the CaM·peptide complex structure does not reveal how the surface of CaM might interact with the rest of the target protein, such interactions are undoubtedly critical for enzyme activation. The very large peptide-induced conformational change in CaM described by Ikura *et al.* (7) and Meador *et al.* (6) will generate new functional domains on the solvent-exposed faces of CaM. These may in turn interact with functional domains on the target enzyme that are distinct from the CaM binding domain. Such additional interactions may help to generate and/or stabilize the active conformation of the target enzyme.

Acknowledgments—We thank Vann Bennett for the use of spectrofluorimeter and J. David Johnson for helpful discussions.

REFERENCES

1. Means, A. R., VanBerkum, M. F. A., Bagchi, I., Lu, K. P., and Rasmussen, C. D. (1991) *Pharmacol. & Ther.* **50,** 255–270
2. Babu, Y. S., Bugg, C. E., and Cook, W. J. (1988) *J. Mol. Biol.* **204,** 191–204
3. Barbato, G., Ikura, M., Kay, L. E., Pastor, R. W., and Bax, A. (1992) *Biochemistry* **31,** 5269–5278
4. Heidorn, D. B., and Trewhella, J. (1988) *Biochemistry* **27,** 909–915
5. Persechini, A., and Kretsinger, R. H. (1988) *J. Biol. Chem.* **263,** 12175–12178
6. Meador, W. E., Means, A. R., and Quiocho, F. A. (1992) *Science* **257,** 1251–1255
7. Ikura, M., Clore, G. M., Gronenborn, A. M., Zhu, G., Klee, C. B., and Bax, A. (1992) *Science* **256,** 632–638
8. Herzberg, O., and James, M. N. G. (1988) *J. Mol. Biol.* **203,** 761–779
9. Strynadka, N. C. J., and James, M. N. G. (1989) *Annu. Rev. Biochem.* **58,** 951–998
10. Kretsinger, R. H. (1987) *Cold Spring Harbor Symp. Quant. Biol.* **52,** 499–510
11. George, S. E., VanBerkum, M. F. A., Ono, T., Cook, R., Hanley, R. M., Putkey, J. A., and Means, A. R. (1990) *J. Biol. Chem.* **265,** 9228–9235
12. Walsh, M. P., Vallet, B., Cavadore, J., and Demaille, J. G. (1980) *J. Biol. Chem.* **255,** 335–337
13. Leavis, P. C., and Kraft, E. L. (1978) *Arch. Biochem. Biophys.* **186,** 411–415
14. Dedman, J. R., Potter, J. D., Jackson, R. L., Johnson, J. D., and Means, A. R. (1977) *J. Biol. Chem* **252,** 8415–8422
15. Johnson, J. D., Collins, J. H., Robertson, S. P., and Potter, J. D. (1980) *J. Biol. Chem.* **255,** 9635–9640
16. VanBerkum, M. F. A., and Means, A. R. (1991) *J. Biol. Chem.* **266,** 21488–21495
17. Horton, R. M., Hunt, H. D., Ho, S. N., Pullen, J. K., and Pease, L. R. (1989) *Gene* **77,** 61–68
18. Putkey, J. A., Sweeney, H. L., and Campbell, S. T. (1989) *J. Biol. Chem.* **264,** 12370–12378
19. Putkey, J. A., Carroll, S. L., and Means, A. R. (1987) *Mol. Cell. Biol.* **7,** 1549–1553
20. Crowe, J. S., Cooper, H. J., Smith, M. A., Sims, M. J., Parker, D., and Gewert, D. (1991) *Nucleic Acids Res.* **19,** 184
21. Sambrook, J., Fritsch, E. F., and Maniatis, T. (1989) *Molecular Cloning: A Laboratory Manual,* Cold Spring Harbor Laboratory Press, Cold Spring Harbor, New York
22. Hanahan, D. (1983) *J. Mol. Biol.* **166,** 557–580
23. VanBerkum, M. F. A., George, S. E., and Means, A. R. (1990) *J. Biol. Chem.* **265,** 3750–3756
24. Grynkiewicz, G., Poenie, M., and Tsien, R. Y. (1985) *J. Biol. Chem.* **260,** 3440–3450
25. Putkey, J. A., Ono, T., VanBerkum, M. F. A., and Means, A. R. (1988) *J. Biol. Chem.* **263,** 11242–11249
26. Grabarek, Z., Grabarek, J., Leavis, P. C., and Gergely, J. (1983) *J. Biol. Chem.* **258,** 14098–14102
27. Grabarek, Z., and Gergely, J. (1983) *J. Biol. Chem.* **258,** 14103–14105
28. Kretsinger, R. H. (1980) *CRC Crit. Rev. Biochem.* **5,** 119–173
29. Reid, R. E., and Hodges, R. S. (1980) *J. Theor. Biol.* **84,** 401–444
30. Reid, R. E. (1985) *J. Theor. Biol.* **114,** 353–374

31. Linse, S., Brodin, P., Johansson, C., Thulin, E., Grundstrom, T., and Forsén, S. (1988) *Nature* **335,** 651–652
32. Linse, S., Johansson, C., Brodin, P., Grundstrum, T., Drakenberg, T., and Forsen, S. (1991) *Biochemistry* **30,** 154–162
33. Sekharudu, Y. C., and Sundaralingam, M. (1988) *Prot. Engineering* **2,** 139–146
34. Pearlstone, J. R., Borgford, T., Chandra, M., Oikawa, K., Kay, C. M., Herzberg, O., Moult, J., Herklotz, A., Reinach, F. C., and Smillie, L. B. (1992) *Biochemistry* **31,** 6545–6553
35. Da Silva, A. C. R., De Araujo, A. H. B., Herzberg, O., Moult, J., Sorenson, M., and Reinach, F. C. (1993) *Eur. J. Biochem.213* 599–604
36. Johnson, J. D., and Potter, J. D. (1978) *J. Biol. Chem.* **253,** 3775–3777
37. Holroyde, M. J., Robertson, S. P., Johnson, J. D., Solaro, R. J., and Potter, J. D. (1980) *J. Biol. Chem.* **255,** 11688–11693
38. Crouch, T. H., and Klee, C. B. (1980) *Biochemistry* **19,** 3692–3698
39. Linse, S., Helmersson, A., and Forsén, S. (1991) *J. Biol. Chem.* **266,** 8050–8054
40. Leavis, P. C., Rosenfeld, S. S., Gergely, J., Grabarek, Z., and Drabikowski, W. (1978) *J. Biol. Chem.* **253,** 5452–5459
41. Kincaid, R. L., Manganiello, V. C., Odya, C. E., Osborne, J. C., Stith-Coleman, I. E., Danello, M. A., and Vaughan, M. (1984). *J. Biol. Chem.* **259,** 5158–5166
42. Wu, Z., Sharma, R. K., and Wang, J. H. (1992) *Adv. Second Messenger Phosphoprotein Res.* **25,** 29–43
43. Bentley, J. K., Kadlecek, A., Sherbert, C. H., Seger, D., Sonnenburg, W. K., Charbonneau, H., Novack, J. P., and Beavo, J. A. (1992) *J. Biol. Chem.* **267,** 18676–18682
44. Walsh, M., and Stevens, F. C. (1977) *Biochemistry* **16,** 2742–2749
45. Walsh, M., and Stevens, F. C. (1978) *Biochemistry* **17,** 3924–3930
46. Putkey, J. A., Draetta, G. F., Slaughter, G. R., Klee, C. B., Cohen, P., Stull, J. T. and Means, A. R. (1986) *J. Biol. Chem.* **261,** 9896–9903
47. Craig, T. A., Watterson, D. M., Prendergast, F. G., Haiech, J., and Roberts, D. M. (1987) *J. Biol. Chem.* **262,** 3278–3284
48. Wang, J. H., Sharma, R. K., and Mooibroek, M. M. (1990) in *Molecular Pharmacology of Cell Regulation* (Houslay, M., and Beavo, J. A., eds) Vol. 2, pp. 19–59, Wiley, New York